https://www.scientificarchives.com/journal/archives-of-proteomics-and-bioinformatics

Archives of Proteomics and Bioinformatics Research Article

Identification of the Molecular Basis of Anti-fibrotic Effects of Soluble Guanylate Cyclase Activator Using the Human Lung Fibroblast

Sunhwa Kim[1*], Ashmita Saigal[1], Weilong Zhao[2], Peyvand Amini[1], Alex M. Tamburino[3], Subharekha Raghavan[4], Maarten Hoek[5#]

[1]Cardiometabolic Disease Biology-Discovery, Merck & Co., Inc., South San Francisco, CA, USA

[2]Scientific informatics, Merck & Co., Inc., South San Francisco, CA, USA

[3]Discovery pGx, Merck & Co., Inc., West Point, PA, USA

[4]Chemistry Capabilities Accelerate Therapeutics, Merck & Co., Inc., Kenilworth, NJ, USA

[5]Cardiovascular, Metabolic, Renal, Ophthalmology Biology-Discovery, Merck & Co., Inc., South San Francisco, CA, USA

[#]Present Address: Maze Therapeutics, South San Francisco, CA USA

[*]Correspondence should be addressed to Sunhwa Kim; sunhwa.kim@merck.com

Received date: September 09, 2020, **Accepted date:** November 11, 2020

Abstract

Idiopathic pulmonary fibrosis (IPF) is an irreversible and progressive fibrotic lung disease. Advanced IPF patients often demonstrate pulmonary hypertension, which severely impairs patients' quality of life. The critical physiological roles of soluble guanylate cyclase (sGC)-cyclic guanosine monophosphate (cGMP) pathway have been well characterized in vasodilation and the corresponding therapies and pathway agonists have shown clinical benefits in treating hypertension. In recent years, many preclinical studies have demonstrated anti-fibrotic efficacy of sGC-cGMP activation in various experimental fibrosis models but the molecular basis of the efficacy in these models are not well understood. Also, sGC pathway agonism has demonstrated encouraging clinical benefits in advanced IPF patients (NCT00517933). Here, we have revealed the novel phosphorylation events downstream of sGC activation in human lung fibroblasts using phosphoproteomics. sGCact A, a potent and selective sGC activator, significantly attenuated more than 2,000 phosphorylation sites. About 20% of phosphorylation events, attenuated by transforming growth factor β (TGFβ), a master regulator of fibrosis, were further dysregulated in the sGCact A co-treated lung fibroblasts. The overall magnitude and diversity of the sGCact A phosphoproteome was extensive. Further investigation would be required to understand how these newly identified changes facilitate human pulmonary fibrosis.

Keywords: Phosphoproteome; Soluble guanylate cyclase activator; Transforming growth factor 1; Fibrosis

Introduction

Idiopathic pulmonary fibrosis (IPF) is an irreversible fibrotic lung disease with unknown etiology [1-3]. Although two approved medications, pirfenidone and nintedanib, are able to slow down lung function decline in IPF patients, many other chronic pathologic conditions such as dyspnea and pulmonary hypertension (PH) and overall disease progression, as measured by progression free survival and established lung fibrosis are not well managed [4]. The median survival rate of IPF patients is 3 to 5 years from diagnosis and particularly, IPF-PH patients show a 3-fold increase in mortality as compared to IPF populations without PH [5,6].

For more than a century, nitrates have been used to treat PH as a vasodilator. However, exogenous NO donors turned out to be limited by increased oxidative stress and tolerance. Thus, current treatment strategies focus on inhibiting the degradation of cGMP by targeting phosphodiesterases (PDE), mainly PDE type 5 (PDE5) and the generation of cGMP by increasing the enzymatic activity of sGC, mainly by sGC activators (sGCact) and stimulators (sGCstim), which agonize the activity of oxidized and reduced forms of sGC enzyme, respectively.

Preclinical benefits of sGC-cGMP pathway activation have been explored in various disease model settings with or without vascular disorders. Accumulated evidence have highlighted novel benefits of the sGC pathway activation in fibrosis and/or inflammation. Both sGCact and sGCstim significantly ameliorated diet- and/or injury-induced steatosis, inflammation, and/or fibrosis in experimental fibrosis models in the liver [7-9], skin [10], and/or kidney [11]. For example, an sGCact, BAY60-2270, significantly slowed down fibrosis progression in a CCl_4-induced liver fibrosis model [7]. Both the level of hydroxyproline, a major component of the collagens (COL) and the areas of fibrosis in liver were significantly lowered. BAY41-2272, an sGCstim significantly delayed bleomycin-induced skin fibrosis by decreasing skin thickness and lowering hydroxyproline levels [10]. Another sGCstim, praliciguat/IW-1973 also significantly reduced high fat diet-induced steatosis, inflammation and fibrosis [8]. These preclinical findings in various organ systems with different insults of injuries strongly suggest a general anti-fibrotic effect of sGC agonism. Indeed, sildenafil, a PDE5 inhibitor, improved diffusing capacity for carbon monoxide test, oxygenation and St. George's Respiratory Questionnaire total score in IPF patients, although no statistically significant benefit was measured in the 6-minute walk distance test [12].

Despite the broad understanding of the molecular basis of the sGC pathway activation in vasodilation, primarily mediated through protein kinase G (PKG) and the activation of its down-stream signaling cascades [13-15], the mechanism of how sGC pathway activation can deliver anti-fibrotic effects is not well defined. Small-scale western blot analyses have identified TGFβ-activated extracellular signal-regulated kinase (ERK) as a target of sGC activator BAY41-2272 or cGMP analogue 8-Bromo-cGMP in primary human and rodent dermal fibroblasts [16].

In the present study, we applied phosphoproteomic technology to unbiasedly obtain broad understanding of the overall sGC activation-induced phosphorylation events in human lung fibroblasts. The singleton effect of a sGC activator and its effect on TGFβ signaling are evaluated and discussed.

Materials and Methods

Cell culture and stimulation

HFL1 (human lung fibroblasts) was purchased from ATCC (CCL-153) and grown up to 10 passages in complete culture media of F12K media (ATCC, 30-2004) containing 10% v/v fetal bovine serum (ATCC, 30-2020). Recombinant human TGFβ was purchased from R&D (240-B-010). TGFβ was incubated with any cells for 30 minutes to 48 hours.

Compound preparation

sGCact A (US Patent Number 8455638 B2) and sGC stimulator (US Patent Number 9365574 B2) were synthesized at Merck & Co., Inc., Kenilworth, NJ, USA. TGFβR inhibitor (SB-525334) was purchased from Sigma Aldrich. All compounds were dissolved in dimethyl sulfoxide (DMSO) to stock concentrations of 10 or 1 mM. The final concentration of DMSO in all experiments did not exceed 0.1% v/v.

Phosphoproteome sample preparation, liquid chromatography (LC), mass spectrometry (MS)

HFL1 cells were used for the experiments. Prior to the experiments, HFL1 cells were cultured in complete culture media for 24 hours and then serum starved for overnight. Post 30 minutes with sGCact A or SB-525334 (10 uM or 1 uM of final concentration, respectively), HFL1 cells were stimulated with recombinant TGFβ at 200 ng/ml (final concentration) for 30 minutes. The cells were quickly washed with ice cold phosphate-buffered saline (Thermo Fisher Scientific, 10010023) and lysed in urea lysis buffer (8 M urea, 75 mM NaCl, 50 mM Tris pH 8.2, 10 mM sodium pyrophosphate, 5 mM EDTA, 5 mM EGTA, 10 mM sodium fluoride, 10 mM b-glycerophosphate, 2 mM sodium orthovanadate, phosphatase inhibitor cocktail 2 and 3 (SIGMA, 1:100 (v/v) and Complete protease inhibitor cocktail tablets (Roche)) on ice. 200 ug of proteins were subjected for LC-MS analyses. The detailed MS sample preparation is given in Supplemental Experimental Procedure. The LC-MS analyses, data processing and analyses were conducted at Evotec with their standard procedures [17-20].

Ingenuity pathway analyses (IPA)

The enriched phosphopeptides, selected by p value and/or fold change (FC) as indicated were uploaded into the IPA software (Qiagen). The Core Analyses function included in the software was used to interpret the data for top canonical pathways.

Compound profiling in BioMAP® diversity plus and fibrosis systems

The study was conducted at DiscoverX, a part of Eurofins with their standard procedures. Briefly, 15 human primary cell-based systems were pre-treated with sGC stimulator or activator for 30 minutes prior to the incubation with dynamic stimuli for additional 24-48 hours. These 15 systems designed to model different aspects of the human body in an *in vitro* format. Tissue fibrosis biology is modeled in a pulmonary (SAEMyoF system) and a renal (REMyoF) inflammation environment, as well as in a simple lung fibroblasts (MyoF). Vascular biology

is modeled in both a Th1 (3C system) and a Th2 (4H system) inflammation environment, as well as in a Th1 inflammatory state specific to arterial smooth muscle cells (CASM3C system). Additional systems recapitulate aspects of the systemic immune response including monocyte-driven Th1 inflammation (LPS system) or T cell stimulation (SAg system), chronic Th1 inflammation driven by macrophage activation (*l*Mphg system) and the T cell-dependent activation of B cells that occurs in germinal centers (BT system). The BE3C system (Th1) and the BF4T system (Th2) represent airway inflammation of the lung, while the MyoF system models myofibroblast-lung tissue remodeling. Skin biology is addressed in the KF3CT system modeling Th1 cutaneous inflammation and the HDF3CGF system modeling wound healing.

Homogeneous time resolved fluorescence (HTRF) analyses

The treated HFL lung fibroblasts were lysed for analysis of SMAD3 pSer423/425 (cat#63ADK025PEH, cat#64ND3PEH; CisBio) and VASP pSer239 (cat#63ADK065PEG, cat#63ADK067PEG; CisBio) and the phosphorylation signals were normalized to the total level of SMAD3 or VASP, respectively. The assays were performed as per manufacturer's instruction and the signal was captured using an Envision plate reader.

RNA isolation and quantitative real-time PCR (qPCR) analysis

RNA was isolated with the RNeasy mini kit (Qiagen) according to the manufacturer's instructions. Synthesis of complementary DNA, real-time PCR followed the manufacturer's instructions. All gene expression results are expressed as fold change relative to the housekeeping genes α-actin, glyceraldehyde 3-phosphate dehydrogenase (gapdh) and/or hypoxanthine-guanine phosphoribosyltransferase (hgprt). TaqMan probes were purchased from Life Technologies.

Statistical analyses

Differences of each treatments were tested for their statistical significance by Mann– Whitney U non-parametric test unless otherwise indicated. p values equal or less than 0.05 were considered significant.

Results

sGC activator significantly attenuated inflammation and fibrosis

To broadly investigate the biological effects of sGC pathway activation, two selective and potent agonists of the sGC enzyme, sGC activator (sGCact A: US patent No. 8455638 B2) and sGC stimulator (US patent No. 9365574 B2), were profiled in primary human cells systems that recapitulate key aspects of various human diseases and pathologic conditions by co-culturing distinct population of cells with dynamic repertoire of stimulation (BioMAP® diversity plus and fibrosis panels).

sGCact A significantly attenuated several pathologic aspects in the pulmonary fibrosis system, which recapitulates pathologic features of chronic inflammation and fibrosis by co-culturing human small airway epithelial cells and lung fibroblasts along with the stimulation of

Biological & Disease Relevance	Readouts
Myofibroblast activation	αSMA, E-cadherin, N-cadherin
Fibrosis related matrix activities	Collagen-I, Collagen-III, Collagen-IV, Decorin, MMP-1, MMP-9, TIMP-1, PAI-1
Tissue remodeling/ wound healing activities	EGFR, Keratin 8/18, tPA, uPA, bFGF, sVEGF
Inflammation-related activities	sIL-6, IL-8, sIL-8, IP-10, ITAC, VCAM-1, M-CSF, MCP-1

"s" denotes soluble readouts measured in the system supernatant. Other readouts are direct cell-associated ELISA measurements.

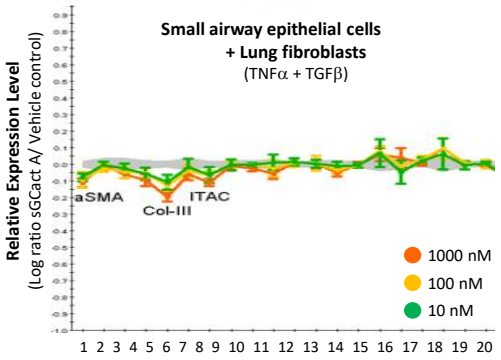

1. αSMA	11. MMP-1
2. CCL2	12. MMP-9
3. VCAM1	13. N-cadherin
4. Collagen-I	14. PAI-I
5. Collagen-III	15. sIL6
6. CXCL10	16. sIL8
7. CXCL11	17. SRB
8. E-cadherin	18. sVEGF
9. EGFR	19. TIMP-1
10. M-CSF	20. uPA

Figure 1: sGC activation-mediated inhibition of fibrosis in human cells. Profiling of sGCact A in BioMAP® Fibrosis panel. X-axes list the quantitative protein marker readouts. Y-axes show log-transformed ratios of readouts. The grey region around the Y-axis represents the 95% significance envelope generated from historical vehicle controls. Biomarker activities are anointed when 2 or more consecutive concentrations change in the same direction relative to vehicle controls, are outside of the significance envelope, and have at least one concentration with an effect size > 20%.

both TGFβ and TNFα (tumor necrosis factor alpha). sGCact A significantly and dose-dependently inhibited α–smooth muscle actin (SMA), COL III and interferon-inducible T cell alpha chemoattractant (ITAC), measuring myofibroblast activation, fibrosis related matrix activities and inflammation-related activities, respectively (Figure 1). In contrast to the pulmonary fibrosis system, the effect of sGCact A in the renal fibrosis system, which contained renal proximal tubule epithelial cells and fibroblasts, only showed decreased matrix metalloproteinase 9 expression (Supplementary Figure 1A). In the BioMAP® diversity panel, sGCact A significantly decreased soluble (s)TNFα and vascular cell adhesion protein (VCAM)-1, measuring inflammation-related activities and plasminogen activator inhibitor (PAI)-1 and tissue inhibitor of metalloproteinases (TIMP)2, measuring tissue remodeling activities in the systems of chronic inflammation and/or autoimmunity conditions (Supplementary Figure 1B). The sGC stimulator also significantly decreased the expression of COL III, αSMA, monocyte chemoattractant protein (MCP)1, and VCAM-1 in renal or pulmonary fibrosis or chronic inflammation conditions (Supplementary Figure 1C). Since the overall effect of sGCact A was more active in the pulmonary fibrosis system as compared to the effect of sGC stimulator, we further continued our studies with sGCact A to investigate its effects in lung fibroblasts.

Interestingly, significantly elevated level of TIMP1, a marker of fibroblast activation, was measured in the MyoF system, treated by either sGCact A or sGCstim (Supplementary Figures 1 A-C). Understanding the mechanistic relationship between sGC agonism and this elevation of TIMP1 protein would be of interest for future studies.

sGC activator-induced changes in cellular phosphoproteomics

sGC agonism decreased ERK phosphorylation in TGFβ-treated dermal fibroblasts. To broaden our understanding of sGC agonism-induced molecular changes, we measured phosphopeptides in the human lung fibroblasts, pretreated with sGCact A and then stimulated with TGFβ. We also pretreated cells with SB-525334, a small molecule compound which abrogates both canonical and non-canonical pathways of TGFβ and inhibits TGFβ-induced fibrosis. The changes from sGCact A and SB-525334 were compared to elucidate any similarities.

The treated HFL1 cells were processed and analyzed by liquid chromatography-mass spectrometry (LC-MS) and MaxQuant program to identify sGCact A-induced changes in phosphopeptides (Figure 2A). The activities of sGCact

A

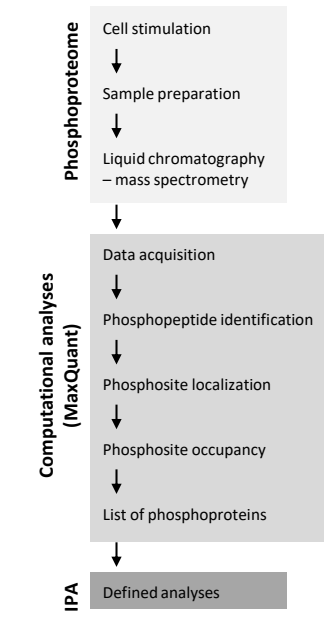

B

Number of phosphorylation sites	Vehicle	SB-525334	sGCact A	Vehicle + TGFβ	SB-525334 + TGFβ	sGCact A + TGFβ
Class I phosphorylation	17589±1641	17594±1639	17592±1640	17595±1637	17593±1639	17591±1640
Compared to Vehicle (FC≥1.5, p≤0.05)	0	28	1675	453	227	1589

C

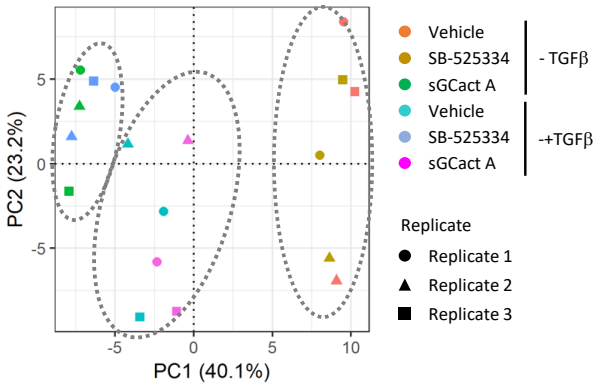

Figure 2: Identification of phosphopeptides, regulated by the sGC activator (sGCact A) in human lung fibroblasts. (A) Workflow for phosphoproteome study. Three independent samples were prepared and processed separately. Post the phosphopeptide identification (FDR at 1%), the data were combined and analyzed at IPA. **(B)** Quantified class I phosphorylation sites across the replicates and the conditions. More than 19,000 class I phosphorylation sites were identified. **(C)** PCA of the acquired data virtual pool normalized intensities. To eliminate the batch effects, the data were normalized to a virtual pool as described at Methods.

A, TGFβ and SB-525334 in lung fibroblasts were assessed prior to LC-MS. TGFβ-induced phosphorylation at Ser423/425 of Smad3 (pSmad3), a primary transcription factor in the canonical TGFβ pathway [21,22], was measured by the HTRF assay (Supplementary Figure 2A). SB-525334 decreased TGFβ-induced pSmad to the basal level ($p<0.01$ as compared to the TGFβ-treated sample). No change was measured in the sGCact-treated cells. In a separate experiment, we confirmed little to no inhibitory effect of sGCactA on TGFβ-induced pSmad2-$Ser^{465/467}$ and pSmad3-$Ser^{423/425}$ (Supplementary Figure 2B). The sGCact A-treatment mildly increased pVASP-Ser^{157} ($p<0.01$ as compared to the vehicle-treated sample), whose phosphorylation was markedly elevated by riociguat, an approved sGC stimulator, in human platelets [23] (Supplementary Figure 2C). The elevation of pVASP-Ser^{157} upon treatment with sGC stimulator was equivalent to the sGCact A effect (data not shown). There was little to no change in VASP phosphorylation events upon TGFβ stimulation with or without SB-525334 (Supplementary Figure 2C).

All treatments quantified similar number of total phosphopeptides with a mean of approximately 17,600 (Figure 2B). A total of 23,885 unique phosphosites were measured from the combined datasets (Supplementary Excel 1). Each treatment significantly attenuated multiple phosphopeptides as compared to those in the vehicle-treated samples (fold change (FC) ≥ 1.5, $p \leq 0.05$; Figure 2B). Almost a 7-fold increase in phosphopeptides were identified from the sGCact A-treated cells (alone or with TGFβ) compared to the cells treated with SB-525334 (alone or with TGFβ) (1632 ± 61 vs 236 ± 213) (Figure 2B). PCA separated and identified two clusters, either treated with sGCact A or TGFβ or none (Figure 2C).

Dynamic changes of TGFβ-induced phosphorylation events by SB-525334

TGFβ stimulation induced dynamic changes in phosphorylation events as shown in the heat map signature (Figure 3A). Overall, TGFβ treatment attenuated a total of 453 phosphopeptide, with 215 up-regulated and 238 down-regulated as compared to vehicle-treated fibroblasts (FC ≥ 1.5, $p \leq 0.05$, Figure 3B and Supplementary Excel 2). As expected, SB-525334 antagonized many TGFβ-induced phosphorylation changes (Figures 3A and 3B). Of the 453 phosphopeptides that showed changes with TGFβ stimulation, co-treatment with SB-525334 resulted in 203 changes in phosphopeptides, with 66 up-regulated and 137 down-regulated as compared to vehicle-treated samples (FC ≥ 1.5, $p \leq 0.05$, Figure 3B).

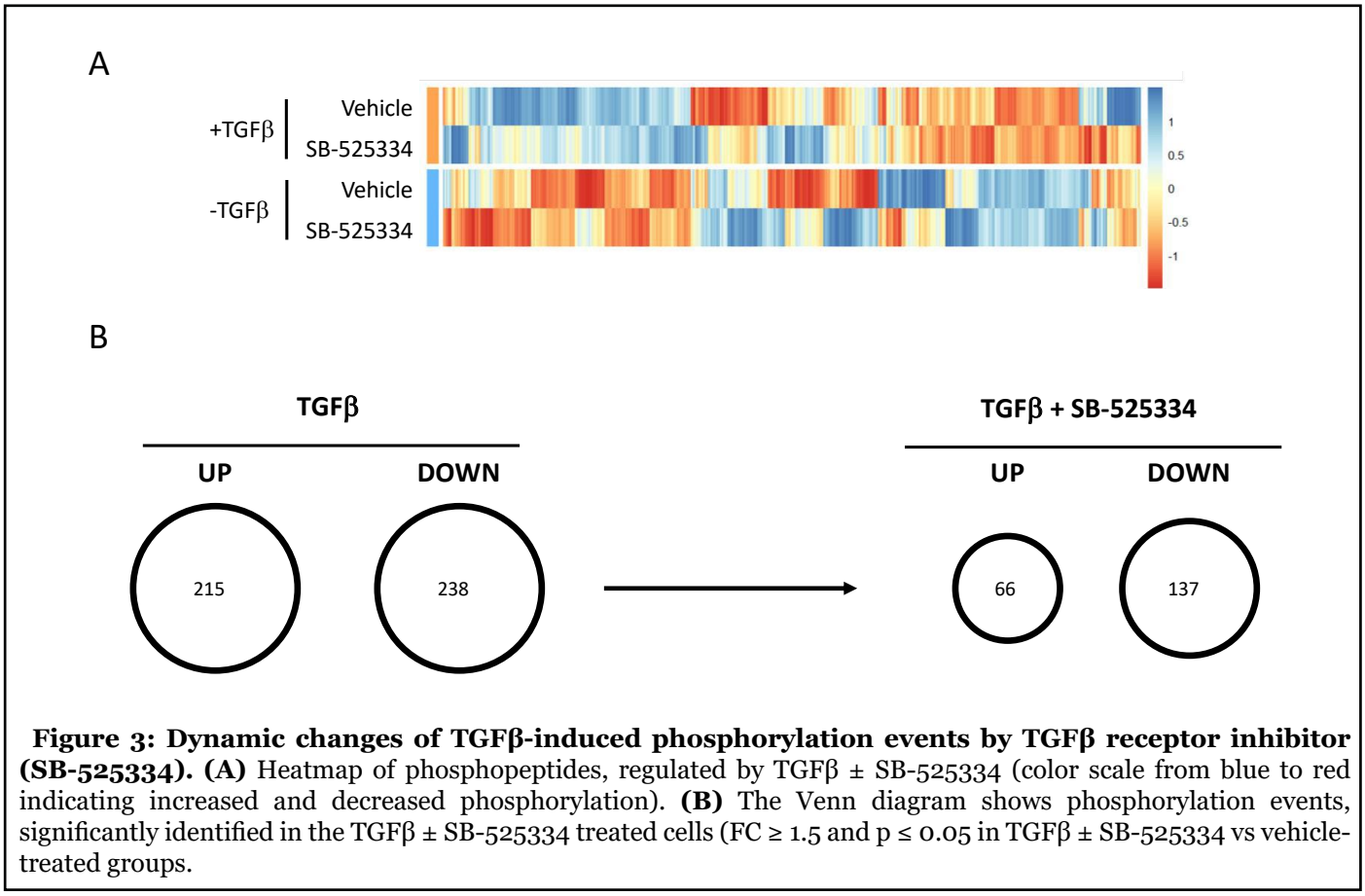

Figure 3: Dynamic changes of TGFβ-induced phosphorylation events by TGFβ receptor inhibitor (SB-525334). (A) Heatmap of phosphopeptides, regulated by TGFβ ± SB-525334 (color scale from blue to red indicating increased and decreased phosphorylation). **(B)** The Venn diagram shows phosphorylation events, significantly identified in the TGFβ ± SB-525334 treated cells (FC ≥ 1.5 and $p \leq 0.05$ in TGFβ ± SB-525334 vs vehicle-treated groups.

Within the phosphopeptides that were changed with SB-525334 co-treatment, 37 phosphopeptides and 16 phosphopeptides showed a decrease and an increase, respectively, of at least 1.5-fold relative to TGFβ treatment alone (Tables 1 and 2).

To identify which TGFβ biological pathways were modulated under different treatment conditions, we ran IPA analyses using the enriched, selected list of significantly changed phosphopeptides (Supplementary Table 1). TGFβ treatment induced phosphopeptides, associated with ERK/mitogen-activated protein kinase (MAPK), ultraviolet (UV)C-induced MAPK and integrin-linked kinase (ILK) pathways. At the same time, TGFβ treatment decreased phosphopeptides, associated with neuregulin, reelin signaling in neurons and signaling by Rho family GTPases pathways. SB-525334 significantly decreased TGFβ-induced associations in ERK/MAP, ILK, p38 MAPK and others (Supplementary Table 1). Some of these pathways are well-studied and -characterized as TGFβ noncanonical pathways and have optimal effects on fibrosis [24,25]. The phosphorylation of Smad2/3 was increased in TGFβ-treated cells (Supplementary Figure 2A). LC-MS was not able to quantify Smad2/3 phosphopeptides (Supplementary Excel 2).

Protein	Gene name	Position	Vehicle	SB-525334	TGFβ	TGFβ+SB-525334
Q9BWH6	RPAP1	Ser268	1.00	1.22	3.07	1.58
Q4ADV7	RIC1	Ser1037	1.00	1.01	3.22	1.72
P26651	ZFP36	Ser186	1.00	0.89	2.66	1.38
P04150	NR3C1	Ser134; Ser45	1.00	0.94	2.10	1.09
Q9NYJ8	TAB2	Ser450	1.00	0.98	2.06	1.06
Q06190	PPP2R3A	Ser181	1.00	0.96	2.44	1.32
P25685	DNAJB1	Ser151	1.00	0.92	1.60	0.82
Q9UPU5	USP24	Ser1281	1.00	1.05	2.29	1.31
P98082	DAB2	Ser723;Thr505	1.00	0.99	2.08	1.19
P04792	HSPB1	Ser78	1.00	0.96	2.01	1.15
Q4ADV7	RIC1	Ser1017	1.00	0.88	1.83	1.04
Q7Z7K6	CENPV	Ser47	1.00	0.73	2.09	1.21
O95816	BAG2	Ser20	1.00	0.84	1.84	1.08
P25685	DNAJB1	Ser149	1.00	0.96	1.58	0.90
Q9NZ32	ACTR10	Thr414	1.00	0.82	1.60	0.94
Q9BZ29	DOCK9	Ser21	1.00	0.82	1.80	1.07
Q15154-5	PCM1	Ser90	1.00	1.04	2.37	1.47
Q9Y6R4-2	MAP3K4	Ser214	1.00	1.01	1.94	1.19
Q86UU0	BCL9L	Ser118	1.00	0.89	1.99	1.23
P04792	HSPB1	Ser82	1.00	0.89	1.73	1.07
P53667	LIMK1	Ser298	1.00	0.93	1.97	1.23
Q4ADV7	RIC1	Ser1040;Ser1003	1.00	0.88	1.89	1.18
A1L020	MEX3A	Ser338	1.00	0.99	1.73	1.09
P78364	PHC1	Ser862	1.00	0.85	1.77	1.12
O15164	TRIM24	Ser1042	1.00	0.73	1.50	0.95
Q08AD1	CAMSAP2	Ser464;Ser453	1.00	1.00	1.70	1.09

Q13769	THOC5	Thr328	1.00	1.00	2.22	1.44
P25054	APC	Ser2533;Ser2432	1.00	1.03	2.03	1.32
Q6KC79-2	NIPBL	Ser1077	1.00	0.99	1.84	1.19
Q9Y4G2	PLEKHM1	Ser482	1.00	0.82	1.65	1.07
P13056	NR2C1	Ser64	1.00	0.92	1.80	1.17
Q9UHB6-4	LIMA1	Ser216	1.00	0.86	1.76	1.15
Q9C0A6	SETD5	Ser591	1.00	0.81	1.73	1.13
Q15154-5	PCM1	Ser93	1.00	0.95	1.80	1.18
O75764	TCEA3	Ser130	1.00	0.83	1.56	1.02
O75151	PHF2	Ser1056	1.00	0.80	2.12	1.40
P18615	NELFE	Ser51;Thr58	1.00	0.91	1.64	1.09

Table 1: TGFβ-increased Phosphopeptides that were antagonized by co-treatment with SB-525334 (FC ≥ 1.5 as compared to TGFβ treatment alone).

Protein	Gene name	Position	Vehicle	SB-525334	TGFβ	TGFβ+SB-525334
Q14118	DAG1	Thr790	1.00	0.84	0.30	0.58
P29317	EPHA2	Ser579	1.00	1.15	0.18	0.39
O75781	PALM	Ser138	1.00	1.07	0.46	0.80
P60468	SEC61B	Ser17	1.00	0.73	0.52	0.85
O43194	GPR39	Ser396	1.00	1.03	0.55	0.89
O00461	GOLIM4	Tyr673	1.00	0.95	0.47	0.76
Q6NZI2	PTRF	Thr279	1.00	0.75	0.40	0.64
Q7Z2K8	GPRIN1	Ser704	1.00	1.17	0.50	0.79
Q8IZD4	DCP1B	Ser283	1.00	1.09	0.53	0.83
P02786	TFRC	Ser24	1.00	0.90	0.30	0.49
P11717	IGF2R	Ser2347	1.00	0.75	0.47	0.73
Q9UN70	PCDHGC3	Ser733	1.00	1.16	0.35	0.55
Q09666	AHNAK	Ser3362	1.00	0.84	0.33	0.51
Q9Y6M7-13	SLC4A7	Ser288;Ser412;Ser279; Ser403	1.00	0.89	0.63	0.95
Q6UVK1	CSPG4	2261	1.00	0.89	0.36	0.55
P43121	MCAM	606	1.00	0.86	0.27	0.40

Table 2: TGFβ -decreased Phosphopeptides that were antagonized by co-treatment with SB-525334 (FC ≥ 1.5 as compared to TGFβ treatment alone).

sGC activator broadly changed phosphorylation events in human lung fibroblasts

sGCact A treatment induced changes in phosphorylation events in the human lung fibroblasts (Figure 4A). A total of 1675 phosphopetides were either increased (n=792) or decreased (n=883) by the treatment of sGCact A alone as compared to the vehicle (FC ≥ 1.5, $p \leq 0.05$, Figure 4B and Supplementary Excel 2). Of the 1675 phosphopeptides that showed changes with sGCact A treatment alone, co-stimulation with TGFβ resulted in 1224 changes in phosphopeptides, with 602 up-regulated and 622 down-

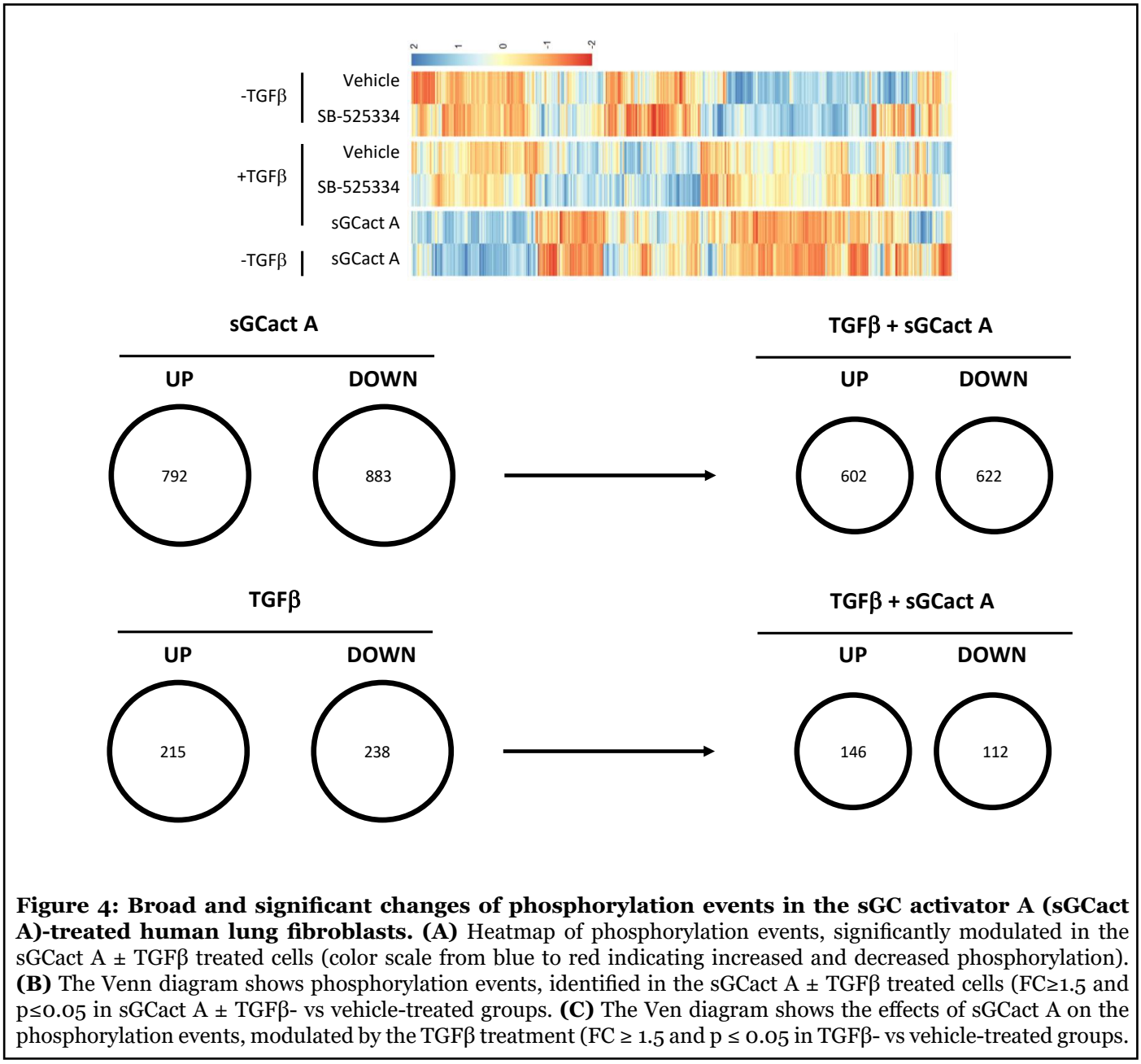

Figure 4: Broad and significant changes of phosphorylation events in the sGC activator A (sGCact A)-treated human lung fibroblasts. (A) Heatmap of phosphorylation events, significantly modulated in the sGCact A ± TGFβ treated cells (color scale from blue to red indicating increased and decreased phosphorylation). **(B)** The Venn diagram shows phosphorylation events, identified in the sGCact A ± TGFβ treated cells (FC≥1.5 and p≤0.05 in sGCact A ± TGFβ- vs vehicle-treated groups. **(C)** The Ven diagram shows the effects of sGCact A on the phosphorylation events, modulated by the TGFβ treatment (FC ≥ 1.5 and p ≤ 0.05 in TGFβ- vs vehicle-treated groups.

regulated as compared to the vehicle-treated samples (FC ≥ 1.5, p ≤ 0.05, Figure 4A). Within the 792 phosphopeptides that showed an increase with sGCact A treatment alone, TGFβ co-treatment decreased 44 phosphorylation events at least 1.5-fold (Table 3). Of the 883 phosphopeptides that showed a decrease with sGCact A treatment alone, TGFβ co-treatment increased only 3 phosphorylation events at least 1.5-fold (Table 4).

To identify which biological pathways were modulated under the treatments of sGCact A, we ran IPA analyses with the list of selected phosphopeptides (Supplementary Excel 2). The IPA analyses identified several affected-pathways (Table 5). sGCact A treatment induced posphopeptides, associated with the signaling pathways of the insulin receptor, B cell receptor and gonadotropin-releasing hormone. sGCact A treatment decreased phosphopeptides associated with signaling in RhoA, GTP-binding protein Ran, protein kinase A (PKA), HIPPO, and polo-like kinase.

Of particular note, the serine/arginine repetitive matrix protein 2 (SRRM2) was identified with the highest number of unique phosphopeptides with sGCA treatment (Table 6). This protein plays an important role in pre-mRNA splicing. A total of 27 individual Ser/Thr phosphorylation sites were significantly decreased in cells upon sGCact A treatment and this inhibition was not altered with TGFβ co-treatment. Among the 27 phosphorylation sites, 16 of

Protein	Gene name	Position	Vehicle	sGCact A	TGFβ	TGFβ+sGCact A
Q9UH99	SUN2	Ser12	1.00	3.81	0.79	1.85
P51149	RAB7A	Ser72	1.00	4.54	0.88	2.41
Q03135	CAV1	Ser37	1.00	2.26	0.74	0.96
Q9Y6M7-13	SLC4A7	Ser26	1.00	3.30	0.82	1.70
Q15035	TRAM2	Ser346	1.00	3.88	0.81	2.11
Q86UL3	AGPAT6	Ser100	1.00	4.75	0.88	2.73
O60238	BNIP3L	Ser166	1.00	4.09	0.82	2.34
Q92685	ALG3	Ser11	1.00	3.88	1.16	2.24
P27824	CANX	Ser583	1.00	2.01	0.62	1.00
P04035	HMGCR	Ser872	1.00	4.34	1.24	2.60
Q9Y210	TRPC6	Ser815	1.00	2.22	0.94	1.22
Q9NQW6	ANLN	Ser485	1.00	4.72	2.82	2.91
Q96S66	CLCC1	Ser438	1.00	2.83	1.06	1.67
O00264	PGRMC1	57	1.00	2.26	1.19	1.30
Q6ZWT7	MBOAT2	474	1.00	3.95	1.21	2.42
P45880	VDAC2	115;104;130	1.00	2.22	0.76	1.27
P16070	CD44	Ser697;Ser295;Thr384;Ser448; Ser623	1.00	3.25	0.80	1.98
Q9Y6M7-13	SLC4A7	Thr263	1.00	2.60	0.78	1.55
P21796	VDAC1	Ser104	1.00	1.91	0.67	1.09
Q92508	PIEZO1	Thr1644	1.00	2.14	0.77	1.25
Q92504	SLC39A7	Ser276	1.00	2.60	0.83	1.59
P11717	IGF2R	Ser2347	1.00	2.14	0.47	1.28
Q9NZJ5	EIF2AK3	Ser1096	1.00	1.84	0.86	1.09
P42167	TMPO	Ser385;Ser276	1.00	2.87	1.03	1.78
Q13563	PKD2	Ser829	1.00	1.87	1.09	1.12
Q09666	AHNAK	Ser5620	1.00	1.72	0.92	1.03
Q92604	LPGAT1	Ser233	1.00	2.50	1.04	1.55
O95292	VAPB	Ser156	1.00	2.96	1.01	1.87
Q9P246-2	STIM2	Ser719	1.00	3.08	1.07	1.95
Q9H3Z4	DNAJC5	Ser12	1.00	1.58	0.73	0.95
Q6PJF5	RHBDF2	Ser385	1.00	2.18	0.82	1.36

Q99442	SEC62	Thr158	1.00	1.72	0.87	1.06
P48651	PTDSS1	Ser442	1.00	2.06	0.87	1.29
O95297	MPZL1	Tyr263	1.00	1.70	0.83	1.05
P38435	GGCX	Ser11	1.00	1.73	0.99	1.09
Q9Y4H4	GPSM3	Ser39	1.00	1.67	1.74	1.06
O00161	SNAP23	Ser110	1.00	1.51	0.84	0.96
P27824	CANX	Ser564	1.00	1.72	0.79	1.10
Q9P0B6	CCDC167	Ser42	1.00	2.42	0.92	1.59
P18031	PTPN1	Ser378	1.00	1.86	0.77	1.22
Q14699	RFTN1	Ser199	1.00	1.53	0.75	1.00
Q14318	FKBP8	Ser296;Ser297	1.00	2.97	1.01	1.96
Q86UE4	MTDH	Ser298	1.00	5.25	1.18	3.49
Q92545	TMEM131	Ser1649	1.00	2.94	1.09	1.96

Table 3: sGCact A-increased Phosphopeptides that were antagonized by co-treatment with TGFβ (FC ≥ 1.5 as compared to sGCact A treatment alone).

Protein	Gene name	Position	Vehicle	sGCact A	TGFβ	TGFβ+sGCact A
P28290	SSFA2	Ser153	1.00	0.37	0.54	0.64
O95391	SLU7	Ser515	1.00	0.34	0.87	0.60
Q15424	SAFB	Ser582	1.00	0.63	0.82	0.98

Table 4: sGCact A-decreased Phosphopeptides that were antagonized by co-treatment with TGFβ (FC ≥1.5 as compared to sGCact A treatment alone).

IPA	Top Canonical Pathways	P value
sGCact A-elevated pathways (n=792, FC ≥ 1.5, p ≤ 0.05)	• Insulin receptor signaling • B cell receptor signaling • GNRH signaling • ErbB signaling • Molecular mechanisms of cancer	• 1.10E-10 • 1.37E-10 • 2.02E-10 • 3.10E-09 • 5.02E-09
sGCact A-lowered pathways (n=883, FC ≥ 1.5, p ≤ 0.05)	• RhoA signaling • RAN signaling • Protein kinase A signaling • HIPPO signaling • Mitotic roles of polo-like kinase	• 4.10E-05 • 6.06E-04 • 6.79E-04 • 9.88E-04 • 1.00E-03

Table 5: Biological pathways that were associated with phosphopeptides in sGCact A treatment.

Protein	Gene name	Site	Vehicle	sGCactA	sGCactA+ TGFβ
		Ser1694	1.00	0.33	0.39
		Ser478*	1.00	0.35	0.41
		Ser518*	1.00	0.43	0.62
		Ser1693	1.00	0.44	0.53
		Ser472*	1.00	0.45	0.50
		Ser783	1.00	0.46	0.62
		Ser1424	1.00	0.48	0.52
		Ser1444	1.00	0.50	0.59
		Ser1582	1.00	0.51	0.58
		Ser1436*	1.00	0.52	0.60
		Ser764*	1.00	0.55	0.69
		Ser456*	1.00	0.56	0.60
		Ser761*	1.00	0.56	0.70
Q9UQ35	SRRM2	Ser231*	1.00	0.57	0.64
		Ser1320	1.00	0.59	0.61
		Ser2694	1.00	0.61	0.62
		Thr1472	1.00	0.61	0.64
		Thr1492	1.00	0.61	0.55
		Ser778	1.00	0.62	0.66
		Thr1511	1.00	0.62	0.71
		Ser1857	1.00	0.63	0.72
		Ser2729*	1.00	0.64	0.66
		Ser1987	1.00	0.64	0.75
		Ser820*	1.00	0.64	0.77
		Ser782*	1.00	0.65	0.66
		Thr2599	1.00	0.66	0.63
		Ser970	1.00	0.66	0.67

Table 6: Unique phosphorylation changes in SRRM2.

these sites were previously known and reported in the UniProt database while 11 phosphorylation sites were newly identified for SRRM2 (marked with * in Table 6).

Dynamic effect of sGC agonism on TGFβ signaling

A total of 453 phosphopeptides were either increased (n=215) or decreased (n=238) by the treatment of TGFβ alone as compared to the vehicle (FC ≥ 1.5, p ≤ 0.05, Figures 3B and 4C and Supplementary Excel 2). Of the 453 phosphopeptides that showed changes with TGFβ stimulation, co-treatment with sGCact A resulted in 258 changes in phosphopeptides, with 146 up-regulated and 112 down-regulated as compared to the vehicle-treated samples (FC ≥ 1.5, p ≤ 0.05, Figure 4C).

Within the phosphopeptides that were changed with sGCact A co-treatment, 10 phosphopeptides and 52 phosphopeptides showed either a decrease or an increase, respectively, of at least 1.5-fold relative to TGFβ treatment alone (Tables 7 and 8). 11 phosphopeptides that were antagonized by sGCactA and TGFβ co-treatment compared to TGFβ treatment alone were also identified in the cells co-treated with SB-525334 and TGFβ (Table 9). The IPA analyses proposed that sGCact A modulated the association of TGFβ-induced changes in the signaling pathways of PKA, Gα12/13 and others (Table 10).

Our study has revealed many novel phosphorylation events, orchestrated by the sGC agonism in human lung fibroblasts as itself or through a cross-talk with TGFβ signaling. The biological implications of these novel findings have not yet been understood. Further studies with genetic and molecular approaches would be warranted.

Protein	Gene name	Position	Vehicle	sGCact A	TGFβ	TGFβ+sGCact A
Q99961	SH3GL1	Ser288	1.00	0.74	1.55	0.61
P15056	BRAF	Ser365	1.00	1.48	2.11	1.12
Q86V48	LUZP1	Thr958	1.00	1.00	1.78	0.94
Q96EY5	MVB12A	Ser188	1.00	0.89	1.58	0.93
P50749	RASSF2	Thr143	1.00	0.96	1.72	1.05
Q8WYP3	RIN2	Ser486	1.00	0.94	1.57	0.97
Q96EQ0	SGTB	Ser297	1.00	0.90	1.50	0.94
Q69YQ0	SPECC1L	Ser113	1.00	1.01	1.67	1.06
Q86V48	LUZP1	Ser995	1.00	1.04	1.65	1.08
P01106	MYC	Ser62	1.00	1.07	1.59	1.06

Table 7: TGFβ-increased Phosphopeptides that were antagonized by co-treatment with sGCact A (FC ≥ 1.5 as compared to TGFβ treatment alone).

Protein	Gene name	Position	Vehicle	sGCact A	TGFβ	TGFβ +sGCact A
P13639	EEF2	Thr57	1.00	1.99	0.45	1.75
Q09666	AHNAK	Ser5773	1.00	1.11	0.29	1.31
Q5M775	SPECC1	Thr114	1.00	1.02	0.49	1.49
P11166	SLC2A1	Ser226	1.00	4.44	0.59	1.59
P11717	IGF2R	Ser2347	1.00	2.14	0.47	1.28
Q09666	AHNAK	Ser5832	1.00	1.55	0.50	1.31
O43194	GPR39	Ser396	1.00	1.32	0.55	1.30
P02786	TFRC	Ser24	1.00	2.07	0.30	0.91
P05556	ITGB1	Thr789	1.00	2.72	0.64	1.37
Q9BYG3	NIFK	Ser145	1.00	1.19	0.53	1.19

P58335-4	ANTXR2	Ser379;Ser276;Tyr381	1.00	1.69	0.46	1.04
P43121	MCAM	Ser606	1.00	1.87	0.27	0.72
Q14118	DAG1	Thr790	1.00	1.39	0.30	0.74
Q13443	ADAM9	Ser752	1.00	1.68	0.38	0.85
P17302	GJA1	Ser306	1.00	1.92	0.47	0.97
P14923	JUP	Thr54	1.00	1.25	0.56	1.09
P25116	F2R	Ser418	1.00	1.36	0.48	0.97
Q6UVK1	CSPG4	Thr2274	1.00	1.69	0.38	0.82
P29317	EPHA2	Ser579	1.00	1.53	0.18	0.52
Q86YV5	SGK223	Ser696	1.00	1.07	0.56	1.08
O43493-2	TGOLN2	Ser70	1.00	1.56	0.63	1.15
P23229-2	ITGA6	Tyr1059	1.00	1.86	0.53	0.98
O95819-6	MAP4K4	Ser811	1.00	1.10	0.65	1.14
P35367	HRH1	Ser271	1.00	1.35	0.39	0.74
P51991-2	HNRNPA3	Ser375	1.00	0.83	0.40	0.75
Q6UVK1	CSPG4	Thr2261	1.00	1.45	0.36	0.69
O95297	MPZL1	Ser260	1.00	1.79	0.54	0.95
Q9UBH6	XPR1	Ser668	1.00	1.63	0.50	0.89
Q13151	HNRNPA0	Ser188	1.00	1.12	0.39	0.71
Q6NZI2	PTRF	Thr279	1.00	0.92	0.40	0.72
Q5T036	FAM120AOS	Ser174	1.00	1.10	0.41	0.73
Q09666	AHNAK	Ser3362	1.00	0.97	0.33	0.60
Q8IUW5	RELL1	Ser224	1.00	1.60	0.48	0.81
Q9Y250	LZTS1	Ser71	1.00	1.16	0.52	0.88
Q14011	CIRBP	Ser130	1.00	1.17	0.64	1.04
P60468	SEC61B	Ser17	1.00	1.16	0.52	0.85
Q9UBG0	MRC2	Ser1453	1.00	1.15	0.32	0.56
P09651	HNRNPA1	Ser368	1.00	0.90	0.41	0.69
O15021	MAST4	Ser1947	1.00	0.87	0.52	0.85
O43491	EPB41L2	Ser87	1.00	0.91	0.44	0.73
Q96RR4	CAMKK2	Ser511	1.00	0.83	0.51	0.83
Q09666	AHNAK	Ser3360	1.00	0.98	0.39	0.64
Q9C004	SPRY4	Ser280	1.00	1.11	0.44	0.71
Q9Y5W9	SNX11	Ser246	1.00	1.21	0.60	0.95
Q14126	DSG2	Ser703	1.00	1.23	0.48	0.76

O15021	MAST4	Ser1446	1.00	0.89	0.66	1.02
Q5UIP0	RIF1	Ser1579	1.00	0.60	0.46	0.73
O00461	GOLIM4	Tyr673	1.00	1.16	0.47	0.74
Q9BTU6	PI4K2A	Ser468	1.00	0.98	0.39	0.59
Q9H1E3	NUCKS1	Ser223	1.00	0.61	0.30	0.46
Q9UIW2	PLXNA1	Ser1619	1.00	0.89	0.25	0.39
Q9Y3C1	NOP16	Ser16	1.00	0.77	0.47	0.70

Table 8: TGFβ-decreased Phosphopeptides that were antagonized by co-treatment with sGCact A (FC ≥ 1.5 as compared to TGFβ treatment alone).

Protein	Gene name	Position	Vehicle	SB-525334	sGCact A	TGFβ	TGFβ+ SB-525334	TGFβ +sGCact A
Q14118	DAG1	Thr790	1.00	0.84	1.39	0.30	0.58	0.74
P29317	EPHA2	Ser579	1.00	1.15	1.53	0.18	0.39	0.52
P60468	SEC61B	Ser17	1.00	0.73	1.16	0.52	0.85	0.85
O43194	GPR39	Ser396	1.00	1.03	1.32	0.55	0.89	1.30
O00461	GOLIM4	Tyr673	1.00	0.95	1.16	0.47	0.76	0.74
Q6NZI2	PTRF	Thr279	1.00	0.75	0.92	0.40	0.64	0.72
P02786	TFRC	Ser24	1.00	0.90	2.07	0.30	0.49	0.91
P11717	IGF2R	Ser2347	1.00	0.75	2.14	0.47	0.73	1.28
Q09666	AHNAK	Ser3362	1.00	0.84	0.97	0.33	0.51	0.60
Q6UVK1	CSPG4	Thr2261	1.00	0.89	1.45	0.36	0.55	0.69
P43121	MCAM	Ser606	1.00	0.86	1.87	0.27	0.40	0.72

Table 9: TGFβ-decreased Phosphopeptides that were antagonized by co-treatment with sGCact A or SB-525334 (FC ≥1.5 as compared to TGFβ treatment alone).

Analyses	Top Canonical Pathways	P-Value
TGFβ-induced phosphopeptides that were antagonized by sGCact A treatment	Acute myeloid leukemia signaling	1.83E-06
	Protein kinase A signaling	2.17E-06
	Ga12/13 signaling	8.30E-06
	Thyroid cancer signaling	1.82E-05
	Cancer drug resistance by drug efflux	2.69E-05
TGFβ-decreased phosphopeptides that were increased by sGCact A treatment	Caveolar-mediated endocytosis signaling	1.17E-04
	Agrin interactions at neuromuscular junction	1.58E-04
	Neuregulin signaling	3.35E-04
	Granulocyte adhesion and diapedesis	3.79E-04
	Virus entry via endocytic pathways	5.06E-04

Table 10: Biological pathways that were associated with TGFβ-induced changes in Phosphopeptides that were antagonized by co-treatment with sGCact A.

Discussion

The sGC enzyme exists in either a reduced or oxidized form in cells and can be pharmacologically activated by sGC stimulator or sGC activator, respectively. Under standard cell culture conditions, it can be assumed that most of the sGC pool would exist in the reduced state and thus sGC stimulator would demonstrate more pronounced effects. However, in our study using the BioMAP® panels with human cells in normal culturing system, sGCact A, a selective and potent sGC activator, showed more activity relative to sGC stimulator in pulmonary fibrosis system and thus we further continued our experiments with sGCact A.

The molecular basis of sGC-cGMP agonism in vasodilation and platelet inactivation have been extensively investigated [13-15]. Several biochemical and molecular studies have revealed its down-stream pathways and critical molecules and modifications in the signaling cascade to enable vascular remodeling and platelet activation. One of the most well-studied and critical molecules in this pathway is PKG, a cGMP-dependent serine/ threonine protein kinase [26,27]. Over 1000 kinase substrates of PKG have been identified and/or proposed based on biochemical analyses, sequence motif searches and *in vitro*/ *in vivo* phosphorylation studies [26,27]. Our study using human lung fibroblasts has also quantified many identified targets of PKG in human platelets [14,15,28-30], *e.g.*, ENSA-Ser^{108}, protein PRRC2A-Ser^{456}, ITPR3-Ser^{1832}, and PDE5-Ser$^{102, 60}$ [14,28] (Supplementary Excel 2). In addition, the totality of the phosphoproteomic data showed the most abundantly quantified phosphorylation events occurred on serine, then followed by threonine phosphorylation. These data suggest PKG activated through sGC agonism plays key roles in lung fibroblasts, analogous to what has been characterized in platelets. However, many validated phosphorylation events on the conserved PKG motif (R/K$_{2-3}$)(X/K)(S/T)X [14] were not identified in the lung fibroblasts. For example, the known PKG-phosphorylation site of ZYX-Ser^{142} (REKV**pS**S) was not identified in our experiment. Instead, Ser259 of ZYX (**pS**P) was decreased and this site was proposed as a substrate of cyclin-dependent kinase (CDK) with a target motif of pS/T-P [31]. In support of CDK activity downstream of sGC agonism in lung fibroblasts, our data also identified increased phosphorylation events at CDK16-Thr^{111} and -Ser^{184}, which correlate with its kinase activity (Supplementary Excel 2). Along this notion, sGCact A-treatment antagonized TGFβ-decreased phosphorylation events on EEF2-Thr57 and SLC2A1-Ser226, which are known targets of EEF2K and protein kinase A (PKA), respectively (Supplementary Excel 2). In addition to PKG and CDK, there are other serine/ threonine-specific protein kinases that play important roles in fibroblasts such as PKA, protein kinase C (PKC), MAPKs, Ca^{2+}/ calmodulin-dependent protein kinases (CaMK). It is still not clear whether PKG is the dominant and major kinase protein under sGC agonism in lung fibroblasts. To better understand key molecules and essential modifications that are involved in sGC agonism-induced anti-fibrotic effects, more comprehensive molecular, biochemical and genetic studies are needed. Limited events of tyrosine phosphorylation were identified (Supplementary Excel 2).

SRRM2 is a large protein with a molecular weight >300 kDa. This protein contains more than 50 serine/ threonine phosphorylation sites; however the regulation and function of these phosphorylation events are not well understood. Our study identified SRRM2 as the most broadly modified protein by the treatment of sGCact A. A total of 27 Ser/Thr phosphorylation events on SRRM2 were decreased upon sGC treatment (Table 6). Previously, two studies quantified changes in phosphorylation events of SRRM2 in the livers from simple steatosis, non-alcoholic steatohepatitis and cancer [32,33]. In these experiments, the phosphorylation events at Thr1003, Ser1083, Thr252, Ser395 and others were increased. Among these changes, two phosphorylation events at Ser1582 and Ser1857, which were increased in liver cancer, were decreased upon sGCact A stimulation in our study. It would be interesting to address any association of these sites in cancer pathology and potential roles of sGC agonism in this process. 11 out of 27 phosphorylation events on SRRM2 were newly identified in our experiment. It would be interesting to investigate any biological implication of these newly identified modifications.

sGCact A agonism decreased TGFβ-induced phosphorylation events. However, its effect on TGFβ-increased phosphorylation events was not robust and only a total of 10 phosphorylation events showed a decrease which was more than 1.5-fold relative to TGFβ treatment alone (Table 7). The association of these proteins to fibrosis is not known. By lowering the cut-off to 1.2-fold, we identified decrease of dual specificity MAPK kinase 2 (MAP2K2)-Ser^{222} and nuclear factor kappa B p105 (NFκB1)-Ser^{907} upon sGCact A and TGFβ co-treatment relative to TGFβ treatment alone (Supplementary Excel 2). ERK was previously identified as a target of sGC agonism in TGFβ-treated dermal fibroblasts [16]. MAP2K2 is a kinase protein, which phosphorylates and subsequently activates ERK [34]. Our experiment showed that sGCact A lowered TGFβ-induced phosphorylation of MAP2K2 (~20% as relative to TGFβ treatment alone) (Supplementary Excel 2). This could imply that the reduction of TGFβ-induced pERK in sGC activator-treated dermal fibroblasts was due to the reduction of pMAP2K2 through sGC agonism.

Also, sGCact A TGFβ co-treatment decreased the phosphorylation event at NFκB1-Ser^{907} relative to TGFβ treatment alone (~20% as relative to TGFβ treatment alone) (Supplementary Excel 2). NFκB1 is an essential molecule to form the NFκB complex, which is a critical transcription factor for inflammatory responses and cell survival [35].

Interestingly but not surprisingly, LC-MS technology was not able to identify the phosphorylation events at the Smad2-Ser$^{465/467}$ and Smad3-Ser$^{423/425}$, which were significantly quantified by HTRF and/or by sandwich ELISA technologies (Supplementary Excel 2). It is uncertain whether HTRF or sandwich ELISA has higher sensitivity than LC-MS. However, several limitations of LC-MS technology have been already discussed elsewhere [36] and raise careful caution for interpreting our data. Also in this study, we have quantified the phosphorylation events but not the expression of total proteins. Although we think there would be limited changes in each protein levels under each condition due to the short treatment time, we cannot rule out a potential impact of differentially modified protein levels on the overall phosphopeptide signals. Careful follow up studies would be warranted.

In conclusion, human lung fibroblast phosphoproteome analyses upon sGC agonism with or without TGFβ co-stimulation have provided a complex picture of sGCact A-induced changes in cellular phosphorylation events. A remarkable number of new phosphorylation sites and changes were quantified in the sGC activator-treated lung fibroblasts and described for the first time. However, the biological implication of many of these changes are still unknown. It would be important to understand how these events facilitate the anti-fibrotic efficacy of sGC agonism. Also, investigation into the biological significance of these sGCact A-induced phosphorylation events in human fibrosis would be warranted.

Conflict of Interest

Sunhwa Kim, Ashmita Saigal, Weilong Zhao, Peyvand Amini, Alex M. Tamburino, Subharekha Raghavan, Saswata Talukdar are employee of Merck Sharp & Dohme Corp., a subsidiary of Merck & Co., Inc., Kenilworth, NJ, USA and stockholder at Merck & Co., Inc., Kenilworth, NJ, USA.

Maarten Hoek was an employee of Merck Sharp & Dohme Corp., a subsidiary of Merck & Co., Inc., Kenilworth, NJ, USA when the study was conducted and is currently an employee of Maze Therapeutics, South San Francisco, CA, USA. Maarten Hoek is a stockholder at Merck & Co., Inc., Kenilworth, NJ, USA.

References

1. Ley B, Collard HR, King Jr TE. Clinical course and prediction of survival in idiopathic pulmonary fibrosis. American Journal of Respiratory and Critical Care Medicine. 2011 Feb 15;183(4):431-40.

2. Nathan SD, Shlobin OA, Weir N, Ahmad S, Kaldjob JM, Battle E, et al. Long-term course and prognosis of idiopathic pulmonary fibrosis in the new millennium. Chest. 2011 Jul 1;140(1):221-9.

3. De Vries J, Kessels BL, Drent M. Quality of life of idiopathic pulmonary fibrosis patients. European Respiratory Journal. 2001 May 1;17(5):954-61.

4. Lederer DJ, Martinez FJ. Idiopathic pulmonary fibrosis. New England Journal of Medicine. 2018 May 10;378(19):1811-23.

5. Nadrous HF, Pellikka PA, Krowka MJ, Swanson KL, Chaowalit N, Decker PA, et al. Pulmonary hypertension in patients with idiopathic pulmonary fibrosis. Chest. 2005 Oct 1;128(4):2393-9.

6. Lettieri CJ, Nathan SD, Barnett SD, Ahmad S, Shorr AF. Prevalence and outcomes of pulmonary arterial hypertension in advanced idiopathic pulmonary fibrosis. Chest. 2006 Mar 1;129(3):746-52.

7. Knorr A, Hirth-Dietrich C, Alonso-Alija C, Härter M, Hahn M, Keim Y, et al. Nitric oxide-independent activation of soluble guanylate cyclase by BAY 60-2770 in experimental liver fibrosis. Arzneimittelforschung. 2008 Feb;58(02):71-80.

8. Flores-Costa R, Alcaraz-Quiles J, Titos E, López-Vicario C, Casulleras M, Duran-Güell M, et al. The soluble guanylate cyclase stimulator IW-1973 prevents inflammation and fibrosis in experimental non-alcoholic steatohepatitis. British Journal of Pharmacology. 2018 Mar;175(6):953-67.

9. Schwabl P, Brusilovskaya K, Supper P, Bauer D, Königshofer P, Riedl F, et al. The soluble guanylate cyclase stimulator riociguat reduces fibrogenesis and portal pressure in cirrhotic rats. Scientific Reports. 2018 Jun 19;8(1):1-3.

10. Beyer C, Reich N, Schindler SC, Akhmetshina A, Dees C, Tomcik M, et al. Stimulation of soluble guanylate cyclase reduces experimental dermal fibrosis. Annals of the Rheumatic Diseases. 2012 Jun 1;71(6):1019-26.

11. Stasch JP, Schlossmann J, Hocher B. Renal effects of soluble guanylate cyclase stimulators and activators:

a review of the preclinical evidence. Current Opinion in Pharmacology. 2015 Apr 1;21:95-104.

12. Idiopathic Pulmonary Fibrosis Clinical Research Network. A controlled trial of sildenafil in advanced idiopathic pulmonary fibrosis. New England Journal of Medicine. 2010 Aug 12;363(7):620-8.

13. Dangel O, Mergia E, Karlisch K, Groneberg D, Koesling D, Friebe A. Nitric oxide-sensitive guanylyl cyclase is the only nitric oxide receptor mediating platelet inhibition. Journal of Thrombosis and Haemostasis. 2010 Jun;8(6):1343-52.

14. Francis SH, Busch JL, Corbin JD. cGMP-dependent protein kinases and cGMP phosphodiesterases in nitric oxide and cGMP action. Pharmacological Reviews. 2010 Sep 1;62(3):525-63.

15. Makhoul S, Walter E, Pagel O, Walter U, Sickmann A, Gambaryan S, Smolenski A, Zahedi RP, Jurk K. Effects of the NO/soluble guanylate cyclase/cGMP system on the functions of human platelets. Nitric Oxide. 2018 Jun 1;76:71-80.

16. Beyer C, Zenzmaier C, Palumbo-Zerr K, Mancuso R, Distler A, Dees C, et al. Stimulation of the soluble guanylate cyclase (sGC) inhibits fibrosis by blocking non-canonical TGFβ signalling. Annals of the Rheumatic Diseases. 2015 Jul 1;74(7):1408-16.

17. Sharma K, D'Souza RC, Tyanova S, Schaab C, Wiśniewski JR, Cox J, et al. Ultradeep human phosphoproteome reveals a distinct regulatory nature of Tyr and Ser/Thr-based signaling. Cell Reports. 2014 Sep 11;8(5):1583-94.

18. Schaab C. Analysis of phosphoproteomics data. Methods in Molecular Biology. 2011;696:41-57.

19. Olsen JV, Blagoev B, Gnad F, Macek B, Kumar C, Mortensen P, et al. Global, in vivo, and site-specific phosphorylation dynamics in signaling networks. Cell. 2006 Nov 3;127(3):635-48.

20. Riley NM, Coon JJ. Phosphoproteomics in the age of rapid and deep proteome profiling. Analytical Chemistry. 2016 Jan 5;88(1):74-94.

21. Souchelnytskyi S, Tamaki K, Engström U, Wernstedt C, Ten Dijke P, Heldin CH. Phosphorylation of Ser465 and Ser467 in the C terminus of Smad2 mediates interaction with Smad4 and is required for transforming growth factor-β signaling. Journal of Biological Chemistry. 1997 Oct 31;272(44):28107-15.

22. Abdollah S, Macı´as-Silva M, Tsukazaki T, Hayashi H, Attisano L, Wrana JL. TβRI phosphorylation of Smad2 on Ser465 and Ser467 is required for Smad2-Smad4 complex formation and signaling. Journal of Biological Chemistry. 1997 Oct 31;272(44):27678-85.

23. Beck F, Geiger J, Gambaryan S, Solari FA, Dell'Aica M, Loroch S, et al. Temporal quantitative phosphoproteomics of ADP stimulation reveals novel central nodes in platelet activation and inhibition. Blood. 2017 Jan 12;129(2):e1-12.

24. Zhang YE. Non-Smad pathways in TGF-β signaling. Cell Research. 2009 Jan;19(1):128-39.

25. Moustakas A, Heldin CH. Non-Smad TGF-beta signals. Journal of Cell Science. 2005 Aug 15;118(Pt 16):3573-84.

26. Tegge W, Frank R, Hofmann F, Dostmann WR. Determination of cyclic nucleotide-dependent protein kinase substrate specificity by the use of peptide libraries on cellulose paper. Biochemistry. 1995 Aug;34(33):10569-77.

27. Dostmann WR, Nickl C, Thiel S, Tsigelny I, Frank R, Tegge WJ. Delineation of selective cyclic GMP-dependent protein kinase Iα substrate and inhibitor peptides based on combinatorial peptide libraries on paper. Pharmacology & Therapeutics. 1999 May 1;82(2-3):373-87.

28. Smolenski A. Novel roles of cAMP/cGMP-dependent signaling in platelets. Journal of Thrombosis and Haemostasis. 2012 Feb;10(2):167-76.

29. Shabb JB. Physiological substrates of cAMP-dependent protein kinase. Chemical Reviews. 2001 Aug 8;101(8):2381-412.

30. Chahdi A, Miller B, Sorokin A. Endothelin 1 induces β1Pix translocation and Cdc42 activation via protein kinase A-dependent pathway. Journal of Biological Chemistry. 2005 Jan 7;280(1):578-84.

31. Dephoure N, Zhou C, Villén J, Beausoleil SA, Bakalarski CE, Elledge SJ, et al. A quantitative atlas of mitotic phosphorylation. Proceedings of the National Academy of Sciences. 2008 Aug 5;105(31):10762-7.

32. Wattacheril J, Rose KL, Hill S, Lanciault C, Murray CR, Washington K, et al. Non-alcoholic fatty liver disease phosphoproteomics: A functional piece of the precision puzzle. Hepatology Research. 2017 Dec;47(13):1469-83.

33. Zhu B, He Q, Xiang J, Qi F, Cai H, Mao J, et al. Quantitative phosphoproteomic analysis reveals key mechanisms of cellular proliferation in liver cancer cells. Scientific Reports. 2017 Sep 7;7(1):10908.

34. Butch ER, Guan KL. Characterization of ERK1 activation site mutants and the effect on recognition by MEK1 and MEK2. Journal of Biological Chemistry. 1996 Feb 23;271(8):4230-5.

35. Demarchi F, Bertoli C, Sandy P, Schneider C. Glycogen synthase kinase-3β regulates NF-κB1/p105 stability. Journal of Biological Chemistry. 2003 Oct 10;278(41):39583-90.

36. de Godoy LM, Olsen JV, de Souza GA, Li G, Mortensen P, Mann M. Status of complete proteome analysis by mass spectrometry: SILAC labeled yeast as a model system. Genome Biology. 2006 Feb 1;7(6):R50.